VERIFICATION OF INTERFACE-TRACKING METHOD WITH MANUFACTURED SOLUTION

Kei Ito and Hiroyuki Ohshima
Fast Reactor Computational Engineering Department
Japan Atomic Energy Agency
4002 Narita, O-arai-machi, Ibaraki, Japan
ito.kei@jaea.go.jp; ohshima.hiroyuki@jaea.go.jp

Tomoaki Kunugi
Department of Nuclear Engineering
Kyoto University
Kyoto daigaku-Katsura, Nishikyo-ku, Kyoto, Japan
kunugi@nucleng.kyoto-u.ac.jp

ABSTRACT

The gas entrainment (GE) due to a hollow vortex has been studied theoretically, experimentally and numerically to establish the design of a sodium-cooled fast reactor which can be operated stably without the core power disturbance caused by entrained bubbles. As a part of the GE study, the authors are developing a high-precision numerical simulation method to evaluate the GE phenomena accurately. The simulation method has been already applied for the simulations of some GE experiments and the simulation results show good agreement with the experimental data. The verification and validation (V&V), however, has not been conducted enough to show the uncertainty of the simulation method because the GE is a highly complicated phenomenon and there are few theoretical and/or experimental data which can be employed for the V&V study. In such a case, the method of manufactured solution (MS) is a promising method to evaluate the numerical error. Few MSs, however, are proposed for the flows with dynamic gas-liquid interface movement due to the difficulty in modeling mathematically the flow-interface interaction. In this paper, the authors develop a new MS which models the GE, i.e. the dynamic interfacial deformation due to a hollow vortex. The MS is considered on an axisymmetric system and radial, circumferential and axial velocities and pressure are formulated to satisfy the continuity equation and the boundary condition on an interface. The interfacial dent grows with time and a gas bubble is generated when the lower part of the interfacial dent is pinched off. The numerical simulation with the authors' high-precision method shows reasonable agreement with the MS in terms of the interfacial dynamic behavior including the bubble pinch-off. In addition, it is confirmed that the simulation accuracy is enhanced by increasing the mesh resolution. Therefore, the developed MS is considered as a good problem for the verification of an interface-tracking method.

KEYWORDS
Gas entrainment, Interface-tracking method, Manufactured solution, Fast reactor

1. INTRODUCTION

The interface-tracking method, e.g. volume-of-fluid method [1-3], level-set method [4,5] or front tracking method [6], is used frequently in recent years to simulate accurately the complicated gas-liquid two-phase flows with large interfacial deformation. The authors also have been developing a two-phase flow simulation code to evaluate the gas (bubble) entrainment phenomena induced by a hollow vortex formed at a cover gas-coolant interface in the reactor vessel of sodium-cooled fast reactors [7-9]. This simulation code uses a high-precision volume-of-fluid method (PLIC-VOF [10,11]) to simulate interfacial dynamic behaviors accurately. In fact, the simulation results of several GE experiments show good agreement with the experimentally observed data, e.g. the GE occurrence mechanism [12,13] or GE flow rate [14]. Therefore, the applicability of the authors' simulation code to the GE phenomena is confirmed by those validation studies.

In these days, systematic verification & validation (V&V) with quantitative numerical error evaluation is required strongly as the responsibility of code developers [15-17]. Therefore, not only the comparison of the simulation results and the experimental data but the fundamental verification is necessary to check the simulation accuracy of each calculation method employed in the code. In particular, the reproducibility of interfacial shape should be confirmed carefully in the V&V of an interface-tracking method. There are some basic problems, e.g. the slotted-disk revolution problem [18,19], known to be employed for suitable verifications. The Kelvin-Helmholtz instability or dam-break problem [20,21] also can be employed for the V&V of the interface-tracking calculation in relatively simplified flows. These simple problems have solutions (a rigorous solution or high-accuracy measurement data) which can be used for the evaluation of the simulation error with the grid convergence test, for example. However, the V&V in realistic flows, e.g. the vortex with the GE in our research, is highly difficult due to the lack of reliable reference data. In usual, there is no suitable verification problem for such complicated flows. Even worth, the experimental measurement of interfacial shape with code V&V quality is difficult when complicated interfacial shape varies rapidly with time.

The method of manufactured solution (MMS) is a promising way to formulate an appropriate verification problem for complicated flows. Even when there is no suitable verification problem due to the complexity of considering flow, a MS can be formulated and used for the code V&V. Therefore, the MMS is used widely in various code V&V studies on single-phase flows. On the other hand, two-phase (interfacial) flows have a moving interface whose modeling is one and primary difficulty in the formulation of the MS for an interfacial flow. In fact, only a few studies on the MMS for two-phase flows [22-24] have been reported as far as the authors know.

In this paper, the authors develop a new MS which models the GE, i.e. the dynamic interfacial deformation due to a hollow vortex. The MS is considered on an axisymmetric system and radial, circumferential and axial velocities and pressure are formulated to satisfy the continuity equation and the boundary condition on an interface. The interfacial dent grows with time and a gas bubble is generated when the lower part of the interfacial dent is pinched off. As the fundamental check of the validity of the formulated MS, numerical simulations are performed with the authors' simulation code and the simulation accuracy is evaluated.

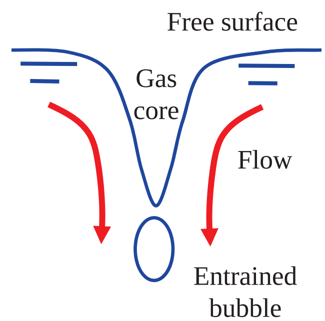

Figure 1. Schematic View of Vortex-type Gas Entrainment.

2. FORMULATION OF MANUFACTURED SOLUTION

In this paper, we formulate a manufactured solution which represents an axisymmetric vortex with a gas core elongated along the vortex core.

2.1. Basic Equations

The basic equations of the manufactured solution are the continuity equation and the axisymmetric (r-θ-z coordinate system) Navier-Stokes equation. It should be noted that the GE is induced by a vortical flow in liquid phase and the influence of gaseous flow is negligible. Therefore, only the liquid region is considered in the manufactured solution.

$$\frac{1}{r}\frac{\partial ru}{\partial r}+\frac{\partial w}{\partial z}=0 \tag{1}$$

$$\frac{\partial u}{\partial t}+u\frac{\partial u}{\partial r}+w\frac{\partial u}{\partial z}-\frac{v^2}{r}=-\frac{1}{\rho}\frac{\partial p}{\partial r}+\upsilon\left(\frac{\partial^2 u}{\partial r^2}+\frac{1}{r}\frac{\partial u}{\partial r}-\frac{u}{r^2}+\frac{\partial^2 u}{\partial z^2}\right)+f_r \tag{2}$$

$$\frac{\partial v}{\partial t}+u\frac{\partial v}{\partial r}+w\frac{\partial v}{\partial z}+\frac{uv}{r}=\upsilon\left(\frac{\partial^2 v}{\partial r^2}+\frac{1}{r}\frac{\partial v}{\partial r}-\frac{v}{r^2}+\frac{\partial^2 v}{\partial z^2}\right)+f_\theta \tag{3}$$

$$\frac{\partial w}{\partial t}+u\frac{\partial w}{\partial r}+w\frac{\partial w}{\partial z}=-\frac{1}{\rho}\frac{\partial p}{\partial z}-g+\upsilon\left(\frac{\partial^2 w}{\partial r^2}+\frac{1}{r}\frac{\partial w}{\partial r}+\frac{\partial^2 w}{\partial z^2}\right)+f_z \tag{4}$$

In Eqs. (2)-(4), υ is the dynamic viscosity, ρ is the liquid density and g is the gravitational acceleration. u, v and w are the velocity components in r, θ and z directions, respectively. The approximate solution of the velocity components is determined in Section 2.2. In addition, f_r, f_θ and f_z show pseudo force in each coordinate direction. They are calculated in Section 2.4. The physical condition at a gas-liquid interface is also considered in the manufactured solution.

$$u_s=\frac{\partial r_s}{\partial t}+w_s\frac{\partial r_s}{\partial z}=\dot{r}_s+w_s r_s' \tag{5}$$

$$p=p_s\left(=p_0\right) \tag{6}$$

The subscript s indicates the values on the interface. r_s is the interface radius from the symmetric axis, which is the equation of z and t. Equation (6) indicate the pressure at the interface is constant (p_0).

2.2. Approximate Solution

As the manufactured solution, the approximate solution of the Navier-Stokes equation has to be determined to satisfy also Eqs. (1) and (5). In the first place, the radial and vertical velocity components are determined.

$$u = -\alpha r_s r_s' r + \alpha \frac{r_s r_s'}{r}\left(2r_s^2 - R^2\right) + \frac{r_s \dot{r}_s}{r} \tag{7}$$

$$w = \alpha\left(r_s^2 - R^2\right) \tag{8}$$

α is a positive constant which determines the magnitudes of the radial and vertical velocity components. R is the radius of the radial boundary and the r_s is defined as $r_s = R$ at the origin of the z direction ($z = 0$) which is the upper limit of the liquid region (see Fig. 3). By substituting Eqs. (7) and (8) into Eq. (1), it is checked that the continuity equation is satisfied.

$$\frac{1}{r}\frac{\partial ru}{\partial r} = -\frac{1}{r}2\alpha r_s r_s' r = -2\alpha r_s r_s'$$
$$\frac{\partial w}{\partial z} = 2\alpha r_s \frac{\partial r_s}{\partial z} = 2\alpha r_s r_s'$$

The first term in the R.H.S. of Eq. (7) is similar to that in the Burgers vortex equation [25]. Therefore, the approximate expression of the circumferential velocity component is determined in reference to the Burgers vortex equation.

$$v = \frac{\Gamma}{2\pi r}\left\{1 - \exp\left(-\frac{r^2}{\lambda}\right)\right\} \tag{9}$$

Γ is the circulation and λ is the characteristics value which determined the vortex velocity distribution.

$$\lambda = \frac{2\upsilon}{\alpha r_s r_s'} \tag{10}$$

To determine the approximation expression of the pressure, the mechanical balance between the gravity and the centrifugal force induced by the circumferential velocity (Eq. (9)) is considered. In addition, Eq. (6) is also considered to satisfy the pressure condition at the interface.

$$\begin{aligned}
&(\mathrm{i})\, z > -L \\
&\quad p = p_0 + \left[1 - \exp\left\{-\beta\left(\frac{r - r_s}{R}\right)^2\right\}\right]\left(-\rho g z - \rho\int_r^R \frac{v^2}{r}\,dr\right) \\
&(\mathrm{ii})\, z < -L \\
&\quad p = p_0 - \rho g z\left[1 - \exp\left\{-\beta\left(\frac{r}{R}\right)^2 + \beta\frac{L + z}{L}\right\}\right]
\end{aligned} \tag{11}$$

β is a positive constant calculated by the pressure value at the radial boundary. L is the depth of the interface, i.e. the gas core length.

2.3. Interfacial Shape

The interfacial shape in the manufactured solution can be determined arbitrarily. In this paper, we employ the following quartic equation.

$$r_s = \frac{9R}{L^4}kz^4 + \frac{24R}{L^3}kz^3 + \frac{R}{L^2}(1+21k)z^2 + \frac{R}{L}(2+6k)z + R \tag{12}$$

k is a function of time, which indicates the ratio of L at each elapsed time to the terminal gas core length (L_{max}). Equation (12) can be rewritten as follows.

$$r_s = \left(\frac{R}{L^2}z^2 + \frac{2R}{L}z + R\right) + k\left(\frac{9R}{L^4}z^4 + \frac{24R}{L^3}z^3 + \frac{21R}{L^2}z^2 + \frac{6R}{L}z\right) \tag{13}$$

The first bracketed term in the R.H.S. of Eq. (13) (quadratic term) represents the fundamental interfacial shape and the second bracketed term (quartic term) represents the interfacial deformation from the fundamental shape, which increase with time. Figure 2 shows the interfacial shape at each elapsed time until the terminal time (t = t_{max}). The interface contracts with time at around z = -0.3 and the interface collapse finally at t = t_{max} to change the interfacial topology and form a gas bubble.

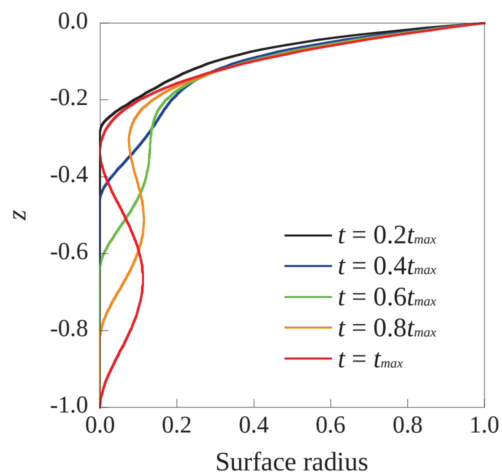

Figure 2. Interfacial Shape Deformation in Manufactured Solution.

It should be mentioned here that Eq. (8) shows the vertical velocity at the gas core tip (r_s = 0) is always αR^2. Therefore, the following relationship has to be satisfied.

$$\dot{L} = \frac{L_{max} - L_{ini}}{t_{max}} = aR^2 \tag{14}$$

L_{ini} is the initial gas core length.

2.4. Pseudo Force

By substituting the approximate solution of the velocity components and pressure (Eqs. (7), (8), (9) and (11)) into the Navier-Stokes equation (Eqs. (2)-(4)), the pseudo force can be calculated as follows.

$$
\begin{aligned}
f_r =& \frac{\partial u}{\partial t} + u\frac{\partial u}{\partial r} + w\frac{\partial u}{\partial z} - \frac{v^2}{r}\exp\left\{-\beta\left(\frac{r-\xi_1}{R}\right)^2 + \beta\frac{\xi_2}{L}\right\} \\
& -\frac{2\beta}{R^2}(r-\xi_1)\left(gz + \int_r^R \frac{v^2}{r}dr\right)\exp\left\{-\beta\left(\frac{r-\xi_1}{R}\right)^2 + \beta\frac{\xi_2}{L}\right\} - \upsilon\frac{\partial^2 u}{\partial z^2}
\end{aligned} \tag{15}
$$

$$
f_\theta = \frac{\partial v}{\partial t} + \left(\alpha\frac{r_s r_s'}{r}\left(2r_s^2 - R^2\right) + \frac{r_s\dot{r}_s}{r}\right)\frac{1}{r}\frac{\partial rv}{\partial r} + w\frac{\partial v}{\partial z} - \upsilon\frac{\partial^2 v}{\partial z^2} \tag{16}
$$

$$
\begin{aligned}
f_z =& 2\alpha r_s\dot{r}_s + 2\alpha^2 r_s r_s'\left(r_s^2 - R^2\right) + g\exp\left\{-\beta\left(\frac{r-\xi_1}{R}\right)^2 + \beta\frac{\xi_2}{L}\right\} \\
& -\left[1-\exp\left\{-\beta\left(\frac{r-\xi_1}{R}\right)^2 + \beta\frac{\xi_2}{L}\right\}\right]\int_r^R \frac{2v}{r}\frac{\partial v}{\partial z}dr \\
& +\beta\left(\frac{2}{R^2}(r-\xi_1)\xi_1' + \frac{\xi_2'}{L}\right)\left(gz + \int_r^R \frac{v^2}{r}dr\right)\exp\left\{-\beta\left(\frac{r-\xi_1}{R}\right)^2 + \beta\frac{\xi_2}{L}\right\} - \upsilon\frac{\partial^2 w}{\partial z^2}.
\end{aligned} \tag{17}
$$

ξ and ξ' are defined as follows.

$$
\begin{aligned}
&\xi_1 = r_s,\quad \xi_2 = 0,\quad \xi_1' = r_s', && z > -L \\
&\xi_1 = 0,\quad \xi_2 = L + z,\quad \xi_2' = 1 && z < -L
\end{aligned} \tag{18}
$$

$\dot{r}_s$ and r_s' are calculated as the derivatives of Eq. (12).

$$
r_s' = \frac{36R}{L^4}kz^3 + \frac{72R}{L^3}kz^2 + \frac{R}{L^2}(2+42k)z + \frac{R}{L}(2+6k) \tag{19}
$$

$$
\dot{r}_s = -\frac{dL}{dt}\left\{\frac{27R}{L^5}kz^4 + \frac{48R}{L^4}kz^3 + \frac{R}{L^3}(2+21k)z^2 + \frac{2R}{L^2}z\right\} \tag{20}
$$

With above pseudo force, the approximate solution satisfies simultaneously the Navier-Stokes equation, continuity equation and physical condition at the interface. Therefore, the determined approximate solution is considered as a manufactured solution. In the study on the verification of a gas-liquid two-phase simulation code, the Navier-Stokes equation with the pseudo force is simulated and the results are compared with the manufactured solution to evaluate the simulation accuracy.

3. INTERFACE-TRACKING SIMULATION

As the fundamental check of the validity of the formulated manufactured solution, numerical simulations are performed with the authors' simulation code in which a high-precision interface-tracking method (PLIC-VOF) is employed to simulate accurately the interfacial dynamic deformation. In addition, physically-appropriate formulations are employed in this code to calculate precisely the mechanical process at the gas-liquid interface, e.g. the surface tension effect. For the application to the gas entrainment simulation in sodium-cooled fast reactors, the unstructured mesh scheme is necessary to model the complicated structural shape at the interface region in the reactors. Therefore, all of the simulation methods employed in the authors' code are developed on arbitrary-shaped unstructured cells, e.g. triangle, tetrahedral or hexahedral cells. Some verification problems, e.g. the slotted-disk revolution problem, have been solved and the simulation results show the authors' code provides superior simulation accuracy to conventional codes both on structured and unstructured meshes.

3.1. Simulation Condition

The simulation domain is a cylindrical region with the height of 1.0 (+ 0.2 for gas region) and the radius of 1.0. As for the boundary conditions, the upper surface is treated as a pressure boundary and the manufactured solution (velocity components and pressure) is applied to the side and bottom boundary faces. In this paper, the initial phase of the verification process for the authors' simulation code is conducted. In other words, the velocity components and pressure in the simulation domain are given as the manufactured solution values and only the interface-tracking simulation is performed.

Two kinds of hexahedral simulation meshes with different mesh resolution are employed in this study. One is a relatively coarse mesh with the representative cell size ratio (h/R) of 0.1 (see Fig. 3) and the other mesh is constructed by subdividing all cells in the coarse mesh equally into eight cells (h/R = 0.05) (see Fig. 4). The simulation results obtained on those two meshes are compared each other to discuss about the simulation accuracy.

Figures 5 and 6 show the velocity and pressure distributions with the interfacial shape in the vertical cross-section at the initial state. The uniform downward velocity is formed at the region below the interfacial dent.

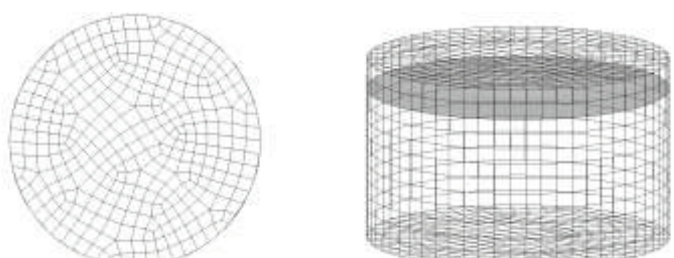

(a) (b)

Figure 3. Simulation Mesh (h/R = 0.1): (a) Top View, (b) Bird's Eye View.

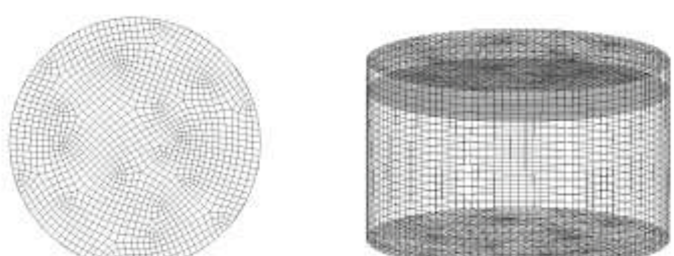

(a) (b)

Figure 4. Simulation Mesh (h/R = 0.05): (a) Top View, (b) Bird's Eye View.

Figure 5. Velocity Distribution in Vertical Cross-Section.

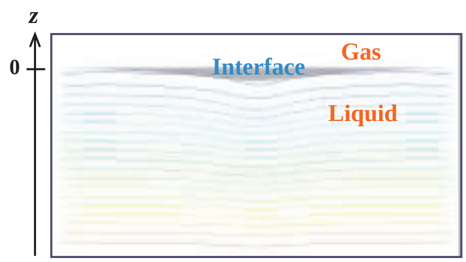

Figure 6. Pressure Distribution in Vertical Cross-Section.

3.2. Simulation Results

Figure 7 shows the simulation result of the interfacial shape deformation with the simulation mesh of h/R = 0.1. Due to the lack of enough mesh resolution, the interfacial radius is larger than the manufactured solution (Fig. 2) especially near the tip of the gas core. However, the interface contraction and resulting bubble formation is obtained even with such a coarse mesh. Figure 8 shows improved simulation results with enhanced mesh resolution compared with the results in Fig. 7. The simulated gas core radius is smaller in this case and the simulation result becomes closer to the manufactured solution.

The numerical error is calculated to evaluate the simulation accuracy quantitatively. The definition of the numerical error at each elapsed time is as follows.

$$E_{L_1} = \frac{1}{n}\sum_{k=1}^{n}\left|\frac{\phi_{calc}^{k} - \phi_{MS}^{k}}{\phi_{ref}}\right| \tag{21}$$

ϕ is the interface radius evaluated at each cell. The subscripts *calc*, *MS* and *ref* indicate the calculated value, manufactured solution and reference value, respectively. Here, the interfacial radius at the origin of z coordinate is employed as ϕ_{ref}, i.e. $\phi_{ref} = 1.0$. The summation is operated for all interfacial cells (n cells) and the superscript k indicates each interfacial cell. Equation (21) provides the L_1 norm of the radial distance error between the calculated interface and the manufactured solution. The L_1 norm is employed here to show the overall numerical error. As shown in Fig. 9, the numerical error increases rapidly at the initial stage until about $t = 0.1t_{max}$. Then, the numerical error shows almost a constant value after $t = 0.25t_{max}$ in the simulation result with the mesh of $h/R = 0.1$. In contrast, the numerical error increases gradually until $t = 0.5t_{max}$ and then, decreases until the terminal state in the simulation result with the mesh of $h/R = 0.05$. The numerical error on the finer mesh is less than half of the error on the coarser mesh except for the short time period around $t = 0.5t_{max}$ and the error ratio at the terminal state is about 0.25. Therefore, the evaluation result of the numerical error implies the simulation accuracy of the interface-tracking method is first to second order.

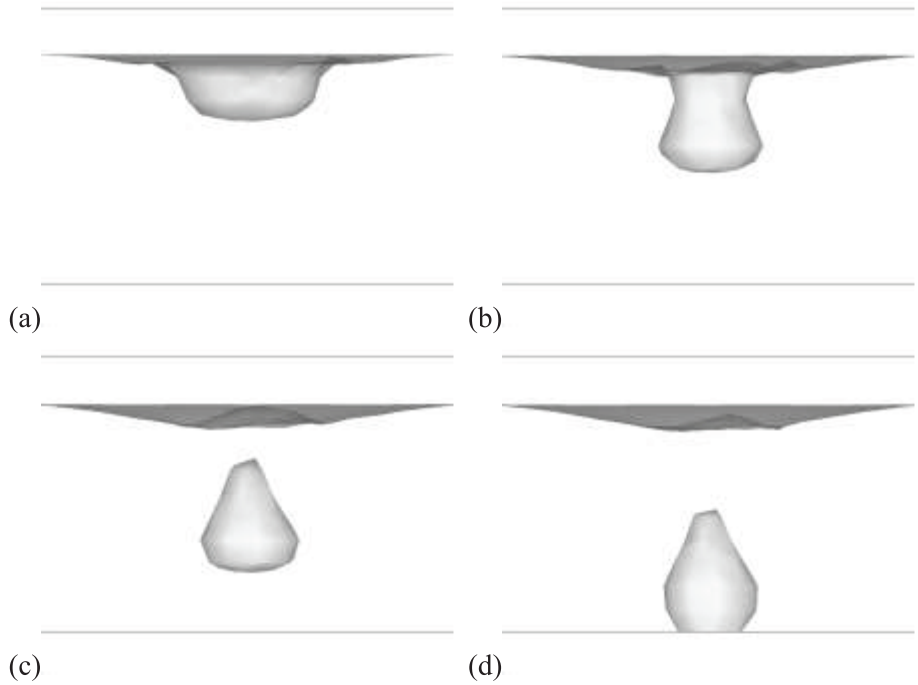

Figure 7. Interfacial Shape Deformation (h/R = 0.1):
(a) $t = 0.25t_{max}$, (b) $t = 0.5t_{max}$, (c) $t = 0.75t_{max}$, (d) $t = t_{max}$.

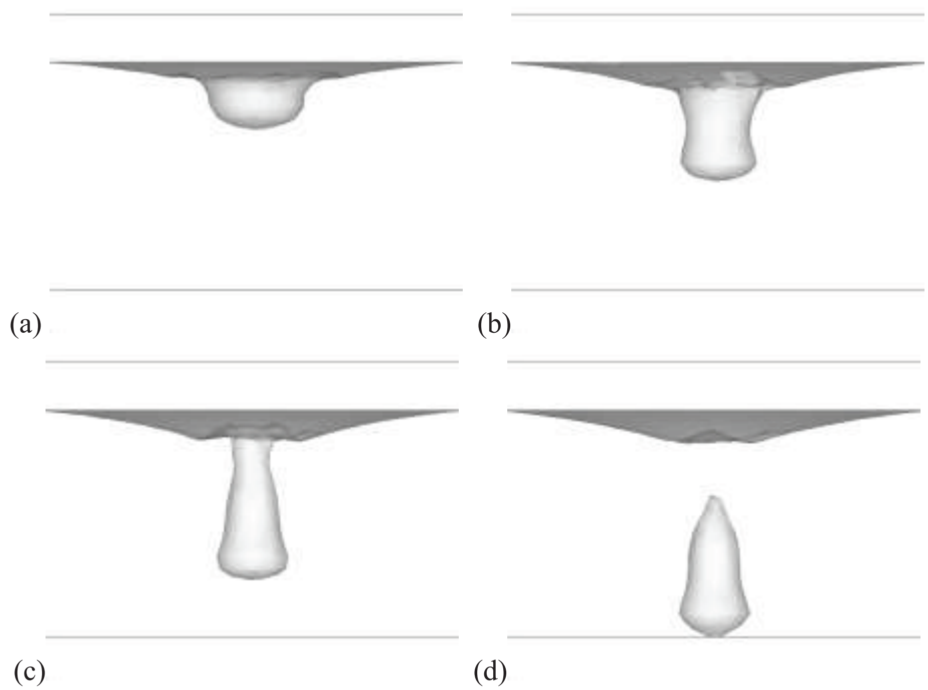

Figure 8. Interfacial Shape Deformation (h/R = 0.05):
(a) $t = 0.25t_{max}$, (b) $t = 0.5t_{max}$, (c) $t = 0.75t_{max}$, (d) $t = t_{max}$.

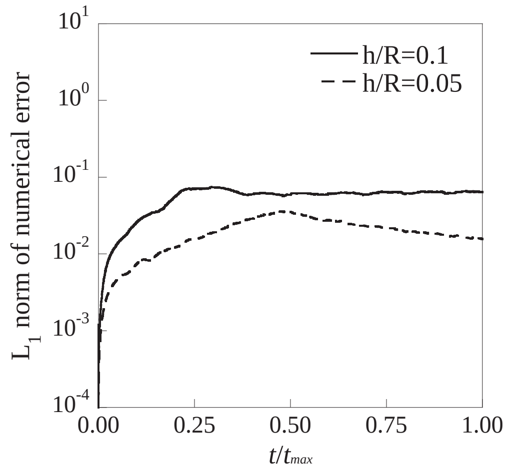

Figure 9. Numerical Error in Interfacial Shape.

4. CONCLUSIONS

In this paper, the authors develop a new MS which models the simplified GE behavior in sodium-cooled fast reactors. Since the GE due to a hollow vortex is considered, the approximate solution of velocity components are determined to be similar to those in the Burgers vortex model. Moreover, the interfacial shape is formulated with a quartic equation which expresses the temporal growth in the interfacial dent and a gas bubble generation (pinch-off) at the terminal state. The numerical simulation with the authors' high-precision method shows reasonable agreement with the MS in terms of the interfacial dynamic behavior including the bubble pinch-off. In addition, it is confirmed that the simulation accuracy is enhanced by increasing the mesh resolution. Therefore, the developed MS is considered as a good problem for the verification of an interface-tracking method.

REFERENCES

1. R. Debar, "A method in two-D Eulerian hydrodynamics," *Technical Report* UCID-19683, Lawrence Livermore National Laboratory, March (1974).
2. W. F. Noh and P. R. Woodward, "SLIC (Simple Linear Interface Calculation)," in: A. I. van der Vooren, P. J. Zandbergen (Eds.), *Lectore Notes in Physics* **59**, Springer-Verlag, New York, pp. 330-340 (1976).
3. C. W. Hirt and D. B. Nichols, "Volume of fluid (VOF) method for the dynamics of free boundaries," *Journal of Computational Physics* **39**, pp. 201-205 (1981).
4. S. Osher and J. A. Sethian, "Fronts propagating with curvature-dependent speed: algorithms based on Hamilton-Jacobi formulations," *Journal of Computational Physics* **79**, pp. 12-49 (1988).
5. M. Sussman, P. Smereka and S. Osher, "A level set approach for computing solutions to incompressible two-phase flow," *Journal of Computational Physics* **114**, pp. 146-159 (1994).
6. G. Tryggvason, B. Burner, A. Esmaeeli, D. Juric, N. Al-Rawahi, W. Tauber, J. Han, S. Nas and Y.-J. Jan, "A front-tracking method for the computations of multiphase flow," *Journal of Computational Physics* **169**, pp. 708-759 (2001).
7. K. Ito, T. Kunugi, H. Ohshima and T. Kawamura, "Formulations and validations of a high-precision volume-of-fluid algorithm on non-orthogonal meshes for numerical simulations of gas entrainment phenomena," *Journal of Nuclear Science and Technology*, **46**, pp. 366-373 (2009).
8. K. Ito, T. Kunugi, H. Ohshima and T. Kawamura, "A volume-conservative PLIC algorithm on three-dimensional fully unstructured meshes," *Computers & Fluids* **88**, pp. 250-261 (2013).

9. K. Ito, T. Kunugi, S. Ohno, H. Kamide and H. Ohshima, "A high-precision calculation methods for interface normal and curvature on an unstructured grid," *Journal of Computational Physics* **273**, pp. 38-53 (2014).
10. D. L. Young, (K. W. Morton and M. J. Baine, ed.), "Numerical methods for fluid dynamics," *Academic Press*, pp. 273-468 (1982).
11. W. Rider and D. B. Kothe, "Reconstructing volume tracking," *Journal of Computational Physics* **141**, pp. 112-152 (1998).
12. N. Kimura, K. Hayashi, M. Igarashi, H. Kamide, M. Itoh and T. Sekine, "Experimental study on flow optimization in upper plenum of reactor vessel for a compact sodium cooled fast reactor," *Nuclear Technology* **152**, pp. 210-222 (2005).
13. K. Okamoto, K. Takeyama and M. Iida, "Dynamic PIV measurement for the transient behavior of a free-surface vortex," *Proceedings of Forth Japan-Korea Symposium on Nuclear Thermal Hydraulics and Safety*, NTHAS4-097, Sapporo, Japan (2004).
14. Y. Koizumi, N. Ohte, H. Kamide, S. Ohno and K. Ito, "Effect of physical properties on gas entrainment rate from free surface by vortex (2nd report)," *Proceedings of 22nd International Conference on Nuclear Engineering*, ICONE22-30959, Prague, Czech Republic (2014).
15. AESJ, "Standard method for safety evaluation using best estimate code based on uncertainty and scaling analysis with statistical approach," *AESJ-SC-S001:2008* (2008).
16. ASME, "Standard for verification and validation in computational fluid dynamics and heat transfer," *ASME V&V 20-2009* (2009).
17. N. Zuber, G. E. Wilson, *et al.*, "An integrated structure and scaling methodology for severe accident technical issue resolution: Development of methodology," *Nuclear Engineering and Design* **186**, pp. 1-21 (1998).
18. S. T. Zalesak, "Fully Multidimensional Flux-Corrected Transport Algorithm for Fluids," *Journal of Computational Physics*, Vol. 31, pp. 335-362 (1979).
19. M. Rudman, "Volume-tracking methods for interfacial flow calculations," *International Journal for Numerical Methods in Fluids* **24**, pp. 671-691 (1997).
20. J. C. Martin and W. J. Moyce, "An experimental study of the collapse of liquid columns on a rigid horizontal plane," *Philosophical Transactions of the* Royal Society *of* London **244**, pp. 312–324 (1952).
21. S. Koshizuka and Y. Oka, "Moving-particle semi-implicit method for fragmentation of incompressible fluid," *Numerical Science of Engineering* **123**, pp. 421-434 (1996).
22. M. Tabata, "Energy stable finite element schemes and their applications to two-fluid flow problems," *European Conference on Computational Fluid Dynamics*, TU Delft, The Netherlands (2006).
23. M. Tabata, "Finite element schemes based on energy-stable approximation for two-fluid flow problems with surface tension," *Hokkaido Mathematical Journal* **36**, pp. 875-890 (2007).
24. M. Tabata, "Numerical simulation of fluid movement in an hourglass by an energy-stable finite element scheme," *Computational Fluid Dynamics Review 2010* (edited by M. M. Hafez, K. Oshima and D. Kwak), Chapter 2, pp. 29-50 (2010).
25. J. M. Burgers, "A mathematical model illustrating the theory of turbulence," *Advance in applied mechanics* (edited by R. Mises and T. Karman), Academic Press ING., New York (1948).